Contents lists available at ScienceDirect

Journal of Molecular Catalysis A: Chemical

journal homepage: www.elsevier.com/locate/molcata

Catalytic oxidation of alkene by cobalt corroles

Li-Ting Huang, Atif Ali, Hua-Hua Wang, Fan Cheng, Hai-Yang Liu*

Department of Chemistry, South China University of Technology, Guangzhou 510640, PR China

ARTICLE INFO

Article history:
Received 5 May 2016
Received in revised form 8 October 2016
Accepted 14 November 2016
Available online xxx

Keywords:
Corrole
Cobalt
Styrene
Catalytic oxidation

ABSTRACT

Four cobalt (III) corroles bearing different number of pentafluorophenyl and phenyl groups were synthesized and characterized by elemental analysis, HR-MS, UV–vis, NMR, XPS as well as cyclic voltammetry. The first investigation of cobalt corrole catalyzed oxidation of alkene was conducted by using styrene as substrate. The best yield was obtained in acetonitrile solvent in the air with TBHP oxidant (96% yield based on oxidant, up to 96 TON). Benzaldehyde was detected as the main product by using PhI(OAc)$_2$, TBHP, KHSO$_5$, PhIO as oxidants. In contrast, styrene oxide was found to be the major product when using *m*-CPBA oxidant. Nearly no products could be found by using H_2O_2 oxidant. Possible catalytic oxidation pathway was also discussed based on the obsewrvations of UV–vis changes of the ctatalytic system in the absence of substrate and in-situ HR-MS.

1. Introduction

Metal corrole has been proved one type of efficient catalysts for oxidation [1]. In fact, lots of metal corroles such as chromium corroles [1], manganese corroles [2–5], and iron corroles [6–9] have been used in the catalytic oxidation of organic substrates. It was found that catalytic oxidation reactions by metal corroles are significantly affected by oxidants, solvents and the electronic structure of the catalysts. Cobalt corrole is a very important class of metal corroles. It is a kind of very promising non-precious-metal catalyst in fuel cell technology and a large number of investigations have been devoted to the catalytic reduction of oxygen by cobalt corroles [10–16].

Cobalt corrole has also been proved as efficient catalysts for cyclopropanation [17], water oxidation [18–21], hydrogen evolution [22–25], CO_2 reduction [26], and photocatalytic water splitting reaction [27]. Cobalt corroles are also potential detection sensor for CO [28–30]. It is well-known that Co(II) porphyrins are an efficient catalysts for the oxidation of alkene [31–34]. To the best of our knowledge, no studies about cobalt corrole catalyzed oxidation of organic substrates has been reported so far. Herein, we wish to report the catalytic oxidation of styrene by cobalt corroles bearing different electronic features (Scheme 1). The effect of solvents and oxidants on the catalytic reactions were also explored.

2. Experimental

2.1. Materials and methods

All chemicals and solvents were purchased from Sinopharm Chemical Reagents Co. Ltd. and used without further purification unless otherwise mentioned. Pyrrole was redistilled prior to use. Commercial analytical grade styrene (Aladdin) was passed through short column of basic alumina prior to use. Iodosylbenzene (PhIO) was synthesized by a reported method [35]. The supporting electrolyte in CV experiments, tetrabutylammonium perchlorate, was purchased from Fluka and recrystallized from ethanol at least three times. The ^{1}H NMR and ^{19}F NMR spectra were recorded at room temperature on a Bruker Avance III 400 spectrometer. X-ray photoelectron spectroscopy (XPS) was performed using an Axis Ultra DLD spectrometer. Mass spectras were taken on Bruker Esquire HCT plus mass spectrometer (ESI/MS) and Bruker maxis impact mass spectrometer with an ESI source (HR-MS). All cyclic voltammograms (CV) were performed in acetonitrile solutions containing 0.1 M TBAP (tetrabutylammonium perchlorate) using an Ingens Model 1030 and cobalt corroles (1×10^{-3} M) under nitrogen atmosphere at ambient temperature. A three-electrode system consisting of a glassy carbon working electrode, a platinum wire counter electrode and Ag/AgCl reference electrode were employed. The scan rate was 100 mV/s. Half-wave potentials ($E_{1/2}$) for reversible or quasi-reversible redox processes were calculated as $E_{1/2} = (E_{pa} + E_{pc})/2$, where E_{pa} and E_{pc} represent the anodic and cathodic peak potentials, respectively. The $E_{1/2}$ value for the ferrocenium/ferrocene couple under these conditions was 0.47 V. The freshly synthesized cobalt corrole solution ($\sim 3 \times 10^{-3}$ M) was taken in the cuvette and

---

* Corresponding author.
E-mail address: chhyliu@scut.edu.cn (H.-Y. Liu).

http://dx.doi.org/10.1016/j.molcata.2016.11.019
1381-1169/

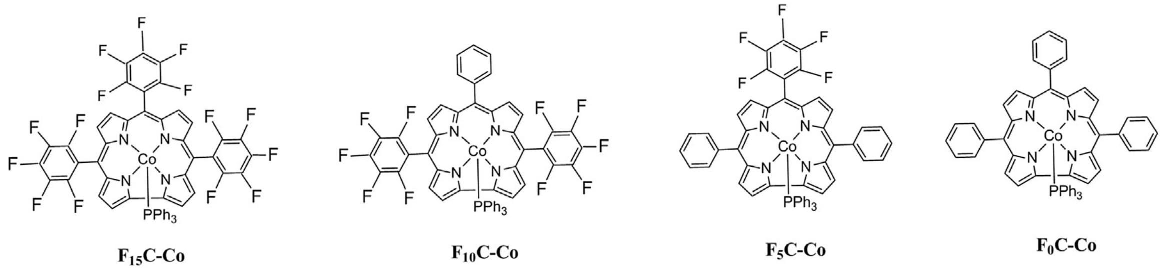

Scheme 1. Structures of cobalt (III) corrole complexes.

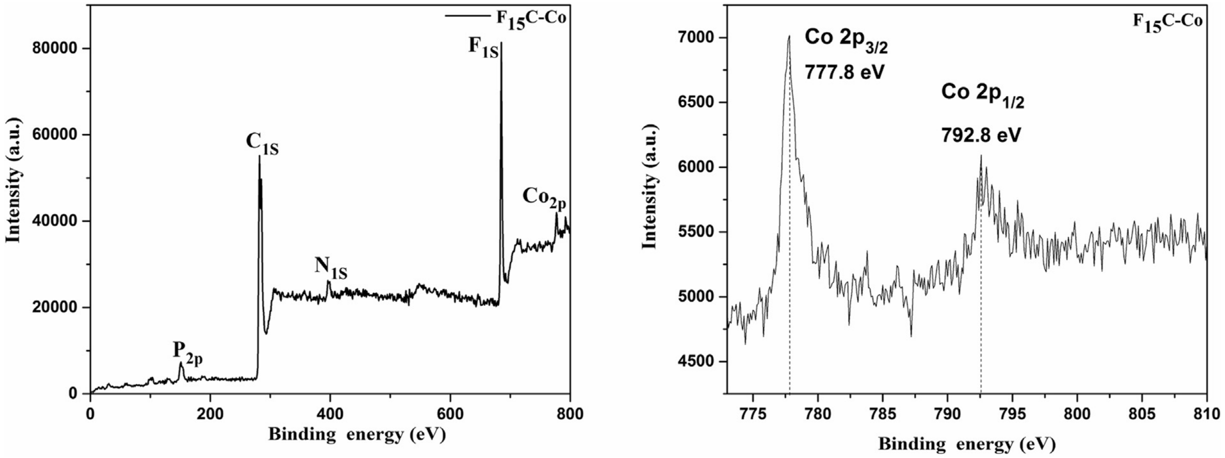

Fig. 1. a (left) X-ray photoelectron spectroscopy of the chemical composition of $\mathbf{F_{15}C\text{-}Co}$ **1b.** (right) Co 2p regions in $\mathbf{F_{15}C\text{-}Co}$.

placed immediately in a thermostat cell holder in a UV–vis spectrophotometer. All experiments, unless specified otherwise, were carried out at room temperature. Electronic absorption measurements were performed on a Blue Star B UV–vis spectrophotometer connected with a thermostat. The absorbance data was collected over the range of 300–800 nm at 5 min interval. Each measurement was repeated three times at 25.0 ± 0.1 °C. The X-band CW EPR test was measured on a Bruker, A300-10-12 Bruker EPR spectrometer (microwave (mw) frequency 9.43 GHz). An mw power of 2.19 mW, a modulation amplitude of 0.4 mT, and a modulation frequency of 100 kHz were used. Measurement was done at a temperature of 103 K.

2.2. Synthesis of freebase corrole

All other A_{3}- and trans-A_2B free base corroles were prepared smoothly according to the reported procedures [6,36–38].

2.3. Synthesis of cobalt (III) corroles

Cobalt corrole $\mathbf{F_0C\text{-}Co}$ was synthesized which follows a method reported in the literature [15]; (5,10,15-tris(pentafluorophenyl) cobalt corrole $\mathbf{F_{15}C\text{-}Co}$ was synthesized according to the literature [39]; New cobalt corroles $\mathbf{F_{10}C\text{-}Co}$, $\mathbf{F_5C\text{-}Co}$ were prepared by 20 mg corresponding free base corrole which was dissolved in 30 mL of ethanol containing 141 mg $CoCl_2{\cdot}4H_2O$, triphenylphosphine (5.0 equivalents vs. the free base corrole) and 30 mg anhydrous NaOAc in 50 mL in a round bottom flask. The mixture was stirred for about for 1.5 h under room temperature and the progress of the reaction monitored by thin-layer chromatography until the starting corrole was consumed. After the completion of reaction, the sample was washed with dichloromethane and water for 2–3 times and was collected. The red fraction was evaporated to dryness and was purified by column chromatography on silica gel (200-300 mesh) using hexene/CH_2Cl_2 as eluent, respectively. The yields of cobalt corroles in all cases were about 75%. All reported ^1H NMR and ^{19}F NMR as well as HRMS-ESI-MS spectra of cobalt corroles were given (see Figs. S1–S11 in the Supporting information).

2.4. 5,10,15-tris (phenyl) cobalt (III) corrole, F0C—Co (III)

UV–vis. (CH_2Cl_2): λ_{max}, nm. ($\times 10^{-3}$ ε, L mol^{-1} cm^{-1}). 385 (42.89), 562 (8.14). HR-MS (ESI): *m*/*z* found: 846.2273, calcd for $C_{55}H_{38}CoN_4P$: 846.2271; ^1H NMR (400 MHz, $CDCl_3$) δ 8.61 (d, *J* = 4.3 Hz, 2H), 8.34 (d, *J* = 4.7 Hz, 2H), 8.16–7.97 (m, 7H), 7.68–7.49 (m, 11H), 7.39 (d, *J* = 7.5 Hz, 1H), 7.06 (t, *J* = 7.3 Hz, 3H), 6.71 (t, *J* = 7.4 Hz, 6H), 4.84–4.66 (m, 6H). Elemental analysis: found (%): C 78.58, H 4.78, N 6.16. calcd for ($C_{55}H_{38}CoN_4P$): C 78.19, H 4.53, N 6.63.

2.5. 5,15-bis (phenyl)-10-(pentafluoropheny) cobalt (III) corrole, F5C-Co (III)

UV–vis. (CH_2Cl_2): λ_{max}, nm. ($\times 10^{-3}$ ε, L mol^{-1} cm^{-1}). 386 (43.72), 556 (6.66), 557 (6.66). HR-MS (ESI): *m*/*z* found: 935.1768, calcd for $C_{55}H_{33}CoF_5N_4P$: 935.1768; ^1H NMR (400 MHz, $CDCl_3$) δ 8.50 (d, *J* = 4.3 Hz, 2H), 8.34 (d, *J* = 4.6 Hz, 2H), 8.05 (d, *J* = 4.5 Hz, 2H), 8.00 (d, *J* = 4.8 Hz, 2H), 7.79 (s, 2H), 7.59 (t, *J* = 6.2 Hz, 8H), 7.49–7.37 (m, 15H); ^{19}F NMR (376 MHz, $CDCl_3$) δ -137.95 (dd, *J* = 395.4, 24.2 Hz), -154.58 (t, *J* = 20.9 Hz), −162.19 to −162.74 (m). Elemental analysis: found (%): C 71.04, H 3.76, N 5.54. calcd for ($C_{55}H_{33}CoF_5N_4P$): C 70.67, H 3.56, N 5.99.

2.6. *5,15-bis (pentafluorophenyl)-10-(phenyl) cobalt (III) corrole, F_{10}C-Co (III)*

UV-Vis. (CH_2Cl_2): λ_{max}, nm. ($\times 10^{-3}$ ε, L mol^{-1} cm^{-1}). 379 (43.19), 408 (38.17), 550 (7.99), 587 (6.70). HR-MS (ESI): *m/z* found: 1047.1123; calcd for $C_{55}H_{28}CoF_{10}N_4NaP$: 1047.1116; ^{1}H NMR (400 MHz, $CDCl_3$) δ 8.69 (d, *J* = 4.2 Hz, 2H), 8.25 (d, *J* = 4.9 Hz, 2H), 8.19 (d, *J* = 4.8 Hz, 2H), 8.00 (d, *J* = 4.5 Hz, 2H), 7.79–7.64 (m, 5H), 7.64–7.32 (m, 15H); ^{19}F NMR (376 MHz, $CDCl_3$) δ -137.04 (dd, *J* = 220.7, 22.7 Hz), −153.71 (dd, *J* = 367.8, 346.9 Hz), −162.23 (dd, *J* = 81.2, 59.1 Hz). Elemental analysis: found (%): C 64.86, H 2.77, N 5.42. calcd for ($C_{55}H_{28}CoF_{10}N_4P$): C 64.46, H 2.75, N 5.47.

2.7. *5,10,15-tris (pentafluorophenyl) cobalt (III) corrole, F_{15}C-Co (III)*

UV-Vis. (CH_2Cl_2): λ_{max}, nm. ($\times 10^{-3}$ ε, L mol^{-1} cm^{-1}). 378 (33.82), 410 (34.14), 550 (5.18), 585 (5.19). HR-MS (ESI): *m/z* found: 1137.0646; calcd for $C_{55}H_{23}CoF_{15}N_4NaP$: 1137.0645; ^{1}H NMR (400 MHz, $CDCl_3$) δ 8.74 (s, 2H), 8.38 (s, 2H), 8.29 (s, 2H), 8.14 (s, 2H), 7.29 (s, 4H), 7.13 (s, 11H); ^{1}F NMR (376 MHz, $CDCl_3$) δ −137.54 (d, *J* = 128.5 Hz), −153.72 (td, *J* = 20.9, 6.2 Hz), −162.12 (dd, *J* = 30.7, 15.3 Hz). Elemental analysis: found (%): 59.56, H 2.12, N 4.99. calcd for ($C_{55}H_{23}CoF_{15}N_4P$): C 59.26, H 2.08, N 5.03.

2.8. *Catalytic oxidation of styrene*

Cobalt corroles **F_{15}C-Co** and **F_0C-Co** have been reported in the literature [15,39], **F_5C-Co** and **F_{10}C-Co** are new compounds. All catalytic reactions were performed at room temperature in 10 mL vessel equipped with a magnetic bar and loaded with catalyst (**F_{15}C-Co**, **F_{10}C-Co**, **F_5C-Co**, **F_0C-Co)** (1 μmol), oxidant (0.1 mmol) and styrene (115 μL, 1 mmol) in solvent (2 mL). After an appropriate reaction time, chlorobenzene (5 μL) was added to this reaction mixture as internal standard. The products were analyzed on an Echrom A90 gas chromatograph equipped with HP-5 capillary column (30.0 m × 320 μm ID; 0.25 μm film thickness) coupled with FID detector. The carrier gas was nitrogen and the chromatographic conditions were as follows: the oven temperature was increased at a rate of 10 °C/min from 60 °C to 250 °C; the injector temperature was set 230 °C; the detector temperature was kept at 250 °C. The injection volume of the filtrated reaction mixture was 1.0 μL and the products were confirmed by the retention time using standard samples at the same GC conditions. The yields of products were reported with respect to the amount of oxidant used.

3. Results and discussion

3.1. *X-ray photoelectron spectroscopy (XPS)*

The XPS survey spectras of the chemical composition of four cobalt corroles are presented in Figs. 1a and S36–S38 in the Supporting information. Fig. 1a shows C, N, P, Co, F in F_{15}C-Co. To further understand the electronic state of cobalt element, high-resolution XPS spectras were examined. The XPS survey of Co 2P region for cobalt corroles are presented in Figs. 1b and S12-S14 in the Supporting information, the binding energy of Co $2P_{3/2}$ and Co $2P_{1/2}$ for F_{10}C-Co, F_{15}C-Co are much higher than that of F_0C-Co, F_5C-Co. Investigation of the XPS spectras of all cobalt corrole revealed similar behavior, Co $2P_{1/2}$ is less intense than Co $2P_{3/2,}$ and the Co 2P core-level spectrum shows two intense peaks. The Co $2P_{3/2}$ binding energy is 777.4 eV in F_0C-Co, 777.3 eV in F_5C-Co, 777.7 eV in F_{10}C-Co, 777.8 eV in F_{15}C-Co, and Co $2P_{1/2}$ binding energy is 793 eV in F_0C-Co(Fig. S12), 792.1 eV in F_5C-Co(Fig. S13), 792 eV in F_{10}C-Co(Fig. S14), 792.6 eV in F_{15}C-Co(Fig. 1b). The result coincides well with the reported data of Co $2P_{3/2}$ [40] and Co $2P_{1/2}$ in cobalt complexes [41–43], revealing that central cobalt is formally in the Co (III) state as reported with previous literature [44].

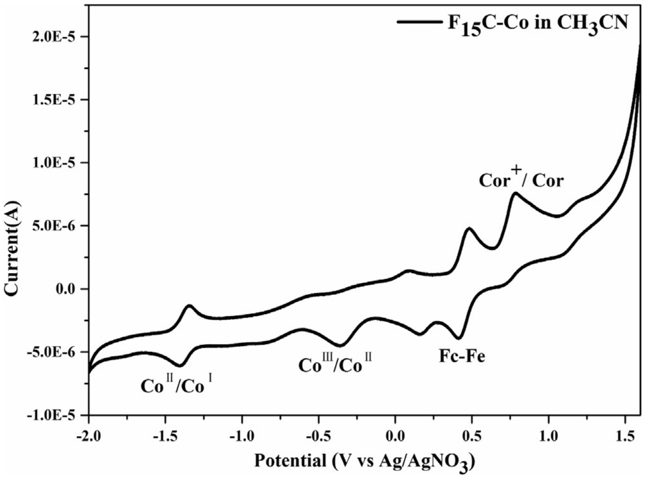

Fig. 2. Cyclic voltammogram of **F_{15}C-Co** in acetonitrile containing TBAP as supporting electrolyte. Scan rate 100 mV/s.

Table 1
Redox potentials (vs. Ag/AgCl) of cobalt (III) corroles in CH_3CN containing TBAP as supporting electrolyte.

Solvent	Corrole	Co^{III}/Co^{II}	Co^{II}/Co^{I}	Cor^{+}/Cor
CH_3CN	F_{15}C-Co	-0.37[a]	-1.38[c]	0.79[b]
	F_{10}C-Co	-0.44[a]	-1.42[a]	0.71[b]
	F_5C-Co	-0.51[a]	-1.55[c]	0.68[b]
	F_0C-Co	-0.73[a]	-1.57[a]	0.60[b]

[a] Irreversible reduction peak potential at a scan rate of 0.1 V/s.

[b] A irreversible oxidation peak potential.

[c] A reversible re-oxidation peak potential ($E_{1/2}$). [d]Fc/Fc couple were measured as 0.47 V under identical conditions.

3.2. *Electrochemistry*

It is apparent that the redox property of cobalt corroles might be the main factor influencing the oxidation of styrene. Thus, to determine the effect of four cobalt corroles with different electron-withdrawing or electron-donating substituents and an axially bound triphenylphosphine ligand on redox property, the electrochemical characteristics of **F_{15}C-Co**(Fig. 2), **F_0C-Co**, **F_5C-Co**, **F_{10}C-Co** (see Figs. S15–S17 in the Supporting information) were examined in CH_3CN (V vs Ag/Ag$^+$) with TBAP (0.1 M) as supporting electrolyte, scan rate = 0.1 Vs^{-1}. The CH_3CN was chosen as a solvent for electrochemical studies of cobalt corroles on the basis of good yield which is based on the oxidant in catalytic oxidation of styrene by cobalt corroles (Table 2).

As shown in Table 1, the first reduction is irreversible in all cases which is in line with previously shown in other five-coordinate cobalt (III) corroles with a bound triphenylphosphine (PPh_3) axial ligand and different substituents on the three *meso*-phenyl rings in CH_2Cl_2 and DMF, which have been reported [15,45]. In the case of CH_3CN, a single one-electron reversible redox couple located at $E_{1/2} = -1.38$ V and one irreversible reduction peak at -0.37 V, with one irreversible peak at 0.79 V were seen for **F_{15}C-Co**. Here, for more electron-deficient cobalt corrole **F_{15}C-Co**, it is more likely that the half-wave potential ($E_{1/2} = -1.38$ V) is attributed to Co^{II}/Co^{I}, the irreversible reduction peak at -0.37 V which may be assigned to Co^{III}/Co^{II}, the irreversibility was distributed to a partial loss of the PPh_3 ligand from $[PPh_3Co^{II}(tpfc)]^-$, which was in agreement with the electrochemical properties of cobalt corrole previously

Please cite this article in press as: L.-T. Huang, et al., J. Mol. Catal. A: Chem. (2016), http://dx.doi.org/10.1016/j.molcata.2016.11.019

Table 2
Oxidation of styrene catalyzed by $\mathbf{F_{15}C\text{-}Co}$ using $PhI(OAc)_2$ in different solvents.

Solvent	Yield (%)[b]					BA[c] Selectivity (%)
	BA	PA	SO	TON	Total	
CH_3CN[a]	73	3	14	90	90	81
DMF	14	2	21	37	37	38
DMAc	7	4	6	17	17	41
DCM	5	2	2	9	9	56

Note: reaction time: 10 h; a using 0.001 mmol catalyst, 0.1 mmol oxidant, 1 mmol styrene (The molar ratio of catalyst/oxidant/styrene was 1/100/1000); b Yields are based on concentration of oxidant; c Selectivity of BA is the percentage of BA in total products.

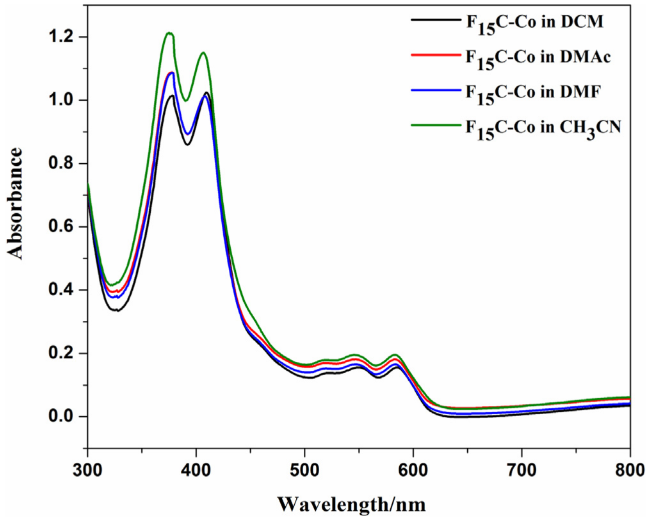

Fig. 3. UV–vis spectra of $\mathbf{F_{15}C\text{-}Co}$ in DCM, DMAc, DMF and CH_3CN at 25.0 ± 0.1 °C.

reported in the literature [26]. The oxidation potentials of four cobalt corroles range from 0.60 V to 0.79 V in CH_3CN may be safely assigned as corrole oxidation (Cor^+/Cor) to Π^- trianions radicals. These results are consistent with the fact that the Co^{II} and Co^{I} forms of the corrole which have been previously reported in the literature [15]. One important finding reflected in Table 1 was that the redox processes were observed for these four cobalt complexes with the Co^{II}/Co^{I}, Co^{III}/Co^{II} and Cor^+/Cor redox couples gradually shifted positively, presumably due to the electron-deficient virtue of the meso-subsitution by phenyl and pentafluorophenyl groups. This was consistent with that the addition of one or more NO_2 groups on the three *meso*-phenyl rings of the triarylcorrole would be expected to shift all redox potentials toward more positive values [46,47]. Similarly, the phenomenon was observed by comparing the cases of reduction potentials of Co complexes of tetrakis (perfluorophenyl) porphyrin [48] and octaethylporphyrin [49], as well as a series of other metal complexes of tpfc and omc [50].

3.3. *UV–vis spectroscopy*

Four cobalt (III) corroles with different electronic stuctures were synthesized and their spectral behavior in four different solvents (DMF, DMAc, DCM, and CH_3CN) were characterized by spectroscopic methods (Fig. 3). In case of these four solvents, the electronic spectras show that $\mathbf{F_{15}C\text{-}Co}$ and $\mathbf{F_{10}C\text{-}Co}$ exhibited similar change (two pronounced Soret bands at 350–450 nm and two weaker absorption in Q-bands in the visible spectral region centered at 550–600 nm), whereas $\mathbf{F_{0}C\text{-}Co}$ exhibited both single Soret band around 400 nm and Q-band around 550–600 nm, which are in accordance with previously reported literature [15,26]. Similarly, UV–vis spectra of $\mathbf{F_{5}C\text{-}Co}$ was almost the same as that of $\mathbf{F_{0}C\text{-}Co}$. UV–vis spectras in various solvents imply that there is no solvent effect on the valent of cobalt corroles.

3.4. *Catalytic activity*

In order to explore the catalytic potential of synthesized cobalt corrole complex, we conducted a series of experiments concerning catalytic oxidation of styrene by (triphenylphosphine) cobalt (III) corroles under different systems. The effect of various solvents and oxidants on the catalytic oxidation were investigated. Styrene is often used as a substrate [51–53]. Using $PhI(OAc)_2$ as oxidant and CH_3CN as solvent gave three products: (1) benzaldehyde, (2) phenylacetaldehyde, and (3) styrene epoxide (Scheme 2).

3.4.1. *Solvent effect*

It has been reported that solvent exerts an effect in the catalytic oxidation reaction [54] and solvent effect in chromium-oxo corroles [55] and molybdenum-oxo corroles [56] has been previously reported. In order to investigate the solvent effect on the reactivity of the cobalt corroles, we used various types of solvents viz. CH_3CN, DMF, DMAc, and dichloromethane (2 mL each) on the oxidation 0.10414 g (1 mmol) of styrene using 0.0322 g (0.1 mmol) $PhI(OAc)_2$ at 40 °C in 10 h. And one salient feature is that yield which is based on oxidant of benzaldehyde using acetonitrile as solvent was much higher than that of the other three solvents. It turned out that acetonitrile was an ideal solvent with the maximum of 90% yield which is based on oxidant, which is in accordance with previous work of our group, showing that acetonitrile is the most suitable solvent for manganese catalyzed oxidation of organic substrate [4,5,57], followed by 37% yield which is based on oxidant of styrene using DMF as a solvent. As the data depicted in Table 2, CH_3CN was selected as the solvent for the optimization of remaining reaction conditions.

3.4.2. *Oxidant effect*

The catalytic data with all the cobalt corroles catalysts using different oxidants was summarized in Table 3A and 3B. Based on the maxmium yield which is based on oxidant (Table 2), acetonitrile was chosen as an ideal solvent. Therefore, we conducted a series of catalytic oxidation of styrene reaction using 1 umol cobalt corroles, 100 equilvalent of six different oxidants viz. $PhI(OAc)_2$, TBHP, H_2O_2, $KHSO_5$, m-CPBA and PhIO, 1000 umol styrene, 2 mL CH_3CN at 40 °C both in the presence and absence of air under the optimized solvent CH_3CN. As seen from Tables 3A and 3B, the yield which is based on oxidant was very low in absence of catalysts. Benzaldehyde was main product along with formation of styrene epoxide and phenylacetaldehyde in CH_3CN when $PhI(OAc)_2$ was used as oxidant. The total yield which is based on oxidant of oxidation of styrene range from 80% to 90% by four kinds of cobalt (III) corroles in CH_3CN using $PhI(OAc)_2$ as oxidant in atmosphere, while it was slightly lower in agron for the four cobalt (III) corroles (77%-85%). Obviously, a significant feature was observed that the selectivity of benzaldehyde was above 80% using four different cobalt corrles as catalysts in the reaction system $PhI(OAc)_2/CH_3CN$ at 40 °C in 10 h in the presence of oxygen. It is clear that cobalt corroles are effective for oxidation of styrene in the presence of $PhI(OAc)_2$. As shown in Table 3A, higher yield of benzaldehyde was obtained in the presence of oxygen than performed in argon atmosphere

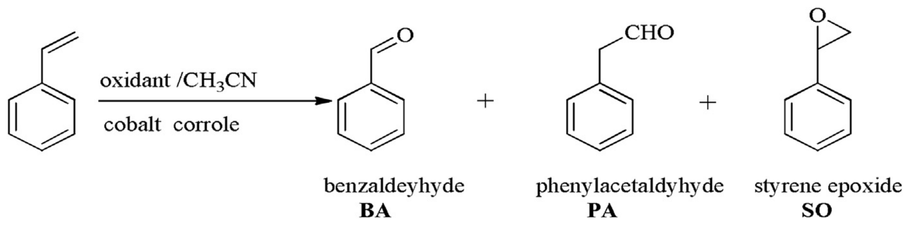

Scheme 2. Oxidation of styrene catalyzed by (triphenylphosphine) cobalt (III) corroles.

Table 3A
Oxidation of styrene catalyzed by cobalt (III) corroles using different oxidants in CH_3CN.

Oxidant	Catalyst	Yield (%)^c					BA^e Selectivity (%)
		BA	PA	SO	TON	Total	
none	F_{15}C-Co	1	0	0	1	1	
$PhI(OAc)_2$^{b}	none	12	1	1	14	14	
	F_{15}C-Co	73 (58)	3 (5)	14 (14)	90 (77)	90 (77)	81 (75)
	F_{10}C-Co	66 (51)	3 (16)	11 (14)	80 (81)	80 (81)	83 (63)
	F_5C-Co	65 (51)	5 (17)	11 (17)	81 (85)	81 (85)	80 (60)
	F_0C-Co	64 (49)	5 (14)	11 (20)	80 (83)	80 (83)	80 (59)
TBHP^a	none	4	0	0	4	4	
	F_{15}C-Co	79 (55)	1 (14)	3 (8)	83 (77)	83 (77)	95 (71)
	F_{10}C-Co	90 (47)	4 (12)	2 (15)	96 (74)	96 (74)	94 (64)
	F_5C-Co	85 (47)	2 (15)	2 (9)	89 (71)	89 (71)	96 (66)
	F_0C-Co	78 (35)	3 (30)	1 (8)	82 (73)	82 (73)	95 (48)
H_2O_2^{d}	none	1	0	0	1	1	
	F_{15}C-Co	1 (1)	0 (0)	0 (0)	1 (1)	1 (1)	100 (100)
	F_{10}C-Co	1 (0)	0 (0)	0 (0)	1 (0)	1 (0)	100
	F_5C-Co	2 (1)	0 (0)	0 (0)	2 (1)	2 (1)	100 (100)
	F_0C-Co	2 (1)	0 (0)	0 (0)	2 (1)	2 (1)	100 (100)

Note: reaction time: 10 h; an Except for 5 h; b using 0.001 mmol catalyst, 0.1 mmol oxidant, 1 mmol styrene (The molar ratio of catalyst/oxidant/styrene was 1/100/1000); c Yields are based on concentration of oxidant; d Yields in parentheses were obtained in agron condition; e Selectivity of BA is the percentage of BA in total products.

Table 3B
Oxidation of styrene catalyzed by cobalt(III) corroles using different oxidants in CH_3CN.

Oxidant	Catalyst	Yield(%)^c					BA^e Selectivity (%)
		BA	PA	SO	TON	Total	
$KHSO_5$	none	10	1	0	11	11	
	F_{15}C-Co	64 (23)	4 (3)	0 (1)	68 (27)	68 (27)	94 (85)
	F_{10}C-Co	78 (58)	6 (6)	0 (0)	84 (64)	84 (64)	93 (91)
	F_5C-Co	46 (18)	7 (3)	0 (2)	53 (23)	53 (23)	87 (78)
	F_0C-Co	27 (13)	3 (7)	2 (0)	32 (20)	32 (20)	84 (65)
PhIO	none	5	0	0	5	5	
	F_{15}C-Co	59 (43)	6 (5)	9 (13)	74 (61)	74 (61)	80 (70)
	F_{10}C-Co	52 (37)	5 (10)	10 (10)	67 (57)	67 (57)	78 (65)
	F_5C-Co	63 (49)	9 (10)	11 (13)	83 (72)	83 (72)	76 (68)
	F_0C-Co	55 (36)	14 (15)	10 (12)	79 (63)	79 (63)	70 (57)
m-CPBA	none	2	9	28	39	39	
	F_{15}C-Co	4 (2)	4 (13)	37 (47)	45 (62)	45 (62)	9 (3)
	F_{10}C-Co	5 (3)	11 (13)	38 (37)	54 (53)	54 (53)	9 (6)
	F_5C-Co	8 (2)	19 (9)	32 (28)	59 (39)	59 (39)	14 (5)
	F_0C-Co	4 (3)	7 (11)	40 (33)	51 (47)	51 (47)	8 (6)

(Table 3A, yields in parentheses), indicating that oxygen plays an important role in formation of benzaldehyde in this reaction. Based on the experimental fact and previously reported literature [4,5], formation of benzaldehyde may be attributed to oxygen free radical catalytic reactions. It is noteworthy that increasing trend in the total yield which is based on oxidant using **F_{15}C-Co** as catalyst is higher than that of other three cobalt corroles in CH_3CN which implies that corrole **F_{15}C-Co** exhibits higher activity in CH_3CN using $PhI(OAc)_2$ as oxidant. The most electron-deficient cobalt corrole gave higher yield of benzaldehyde and higher total yield which is based on oxidant. This was probably due to the electron-withdrawing effect.

It is noteworthy that using TBHP as oxidant, main product was benzaldehyde as indicated by GC analysis, a significant increase in the total yield which is based on oxidant of oxidation products was observed (82%–96%) (See Table 3A) even in five hours, this fact indicates that cobalt corroles work effectively in CH_3CN according to the control experiment with TBHP as oxidant.

However, all the four different cobalt corroles hardly worked in CH_3CN using H_2O_2 as oxidant, because only a small trace of benzaldehyde could be traced, and no other products were found (Table 3A), revealing that the four cobalt corrole catalysts exhibited the least activity on the styrene oxidation in CH_3CN.

During the oxidation of styrene using $KHSO_5$ as oxidant, similar result was obtained as using $PhI(OAc)_2$. In other words, main product was benzaldehyde and the selectivity of benzaldehyde was above 80%. From the date reflected in Table 3B in parentheses, when the reaction was performed in agron, the yield of benzaldehyde which is based on oxidant was significantly decreased.

Similar to the catalytic system with $PhI(OAc)_2$ and $KHSO_5$ as oxidant, an obvious finding was that benzaldehyde was the main

Please cite this article in press as: L.-T. Huang, et al., J. Mol. Catal. A: Chem. (2016), http://dx.doi.org/10.1016/j.molcata.2016.11.019

product using PhIO as oxidant, with significantly higher total yield which is based on oxidant in CH_3CN (67%–83%) (Table 3B). This result was contrary to that of catalytic oxidation of styrene by N-confused manganese porphyrin [5]. Interestingly, benzaldehyde was main product in the cobalt/PhIO/CH_3CN system, whereas iron corroles exhibit different activity on the styrene catalytic oxidation using PhIO as oxidant in CH_3CN [58], which greatly improve the yield which is based on oxidant of styrene epoxide using iron corroles as catalyst.

We can observe that there is a big difference in product profile during oxidation of styrene with Co-corrole/$PhI(OAc)_2$ and Co-corrole/PhIO. $PhI(OAc)_2$ has been used as a mild oxygen source [59–61], thus, $PhI(OAc)_2$ has advantage in enhancing corrole catalyst stability against the oxidation degradation. This is particularly beneficial for metallocorrole-catalyzed oxidations because metallocorroles are less robust and prone to oxidative degradation. PhIO has greater oxidizing power, it may react with cobalt corrole to form reactive metal-oxo species directly, which might accelerate the degradation of the cobalt (III) corrole catalysts, and finally results the decrease of total product yield which is based on oxidant.

Interestingly, as in the case of the *m*-CPBA/CH_3CN system, with catalytic data in Table 3B, styrene epoxide was the main product rather than benzaldehyde. The formation of styrene epoxide may consistent with the previous literature [62,63]. And compared with other oxidants, this is a big difference.

For comparison, additional tests on simple Co (II) salts ($Co(OAc)_2{\cdot}4H_2O$) as catalyst for the homogeneous oxidation of styrene, $V_{CH3CN}/V_{water} = 3:1$ as solvent because simple Co (II) salts are not soluble in CH_3CN and blank tests without any catalyst under the identical conditions have been carried out. And the catalytic data is listed in Tables 3A to 3C. From the data reflected in Table 3C, the total yield which is based on oxidant range from 1%-14% at atmosphere, which is much lower than that of using cobalt corrole as catalyst. In other words, $Co(OAc)_2{\cdot}4H_2O$ shows little activity towards styrene oxidation. Here, we did not perform tests on simple Co (III) salts because they are not stable in the room temperature, which is not suitable in this catalytic system (the reaction temperature is 40 °C).

When the substrate and oxidant are used in a 1:1 ratio (using 0.1 mmol oxidant, 0.1 mmol styrene) with 0.001 mmol **F_{15}C-Co** as catalyst under the identical experimental conditions, we found that the total yield which is based on oxidant range from 1%-10% (the data is not provided), which is much lower than using substrate and oxidant are used in a 10:1 ratio.

3.4.3. Mechanistic considerations

To better understand the efficiency of the catalytic system and to gain futher information about the role of high-valent cobalt corroles on the oxidation of styrene, the UV–vis spectras of the four cobalt corroles in absence of organic substrate with several equilvalents amount of oxidant added were carried out. The UV-Vis spectras of four cobalt complexes upon addition of large excess of oxidants viz. $PhI(OAc)_2$, TBHP, $KHSO_5$, PhIO, m-CPBA were examined every five minutes are shown in the following (Figs. 4 to 9). UV–vis spectras of catalytic reaction mixture when the substrate and oxidant is used in a 1:1 ratio (using 0.1 mmol oxidant, 0.1 mmol styrene) with 0.001 mmol **F_{15}C-Co** as catalyst in CH_3CN under the identical experimental conditions were performed (see Fig. S39-S44 in the Supporting information).

Figs. 4 and S21–S23 in the Supporting information exemplified that an obvious characteristic of weaker Soret band at around 350–450 nm and loss in intensity of Q bands at around 550–600 nm when 8.5 equivalents of $PhI(OAc)_2$ was added to solution with four cobalt corroles in CH_3CN at 25 °C. During the process, we could observe that red cobalt corroles in CH_3CN converted into other

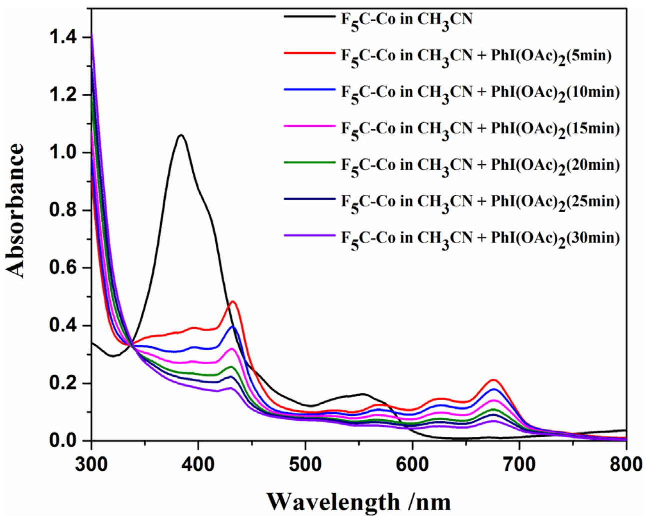

Fig. 4. UV–vis spectral change upon addition of $PhI(OAc)_2$ (8.5 equiv) to a solution of **F_5C-Co** in CH_3CN at 25 °C.

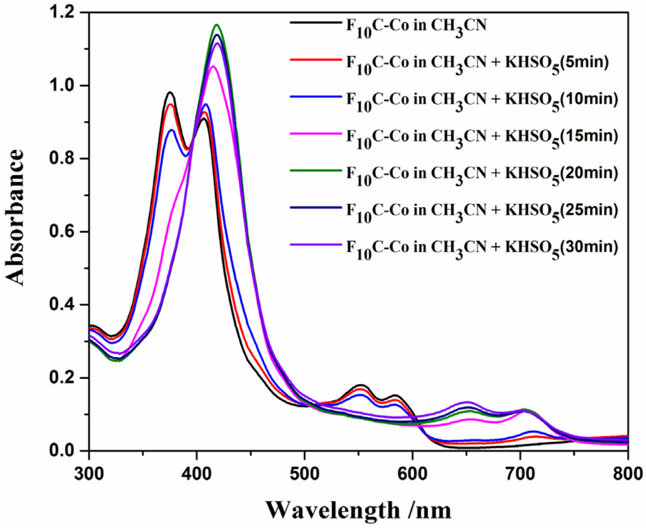

Fig. 6. UV–vis spectral change upon addition of $KHSO_5$ (8.5 equiv) to a solution of **F_{10}C-Co** in CH_3CN at 25 °C.

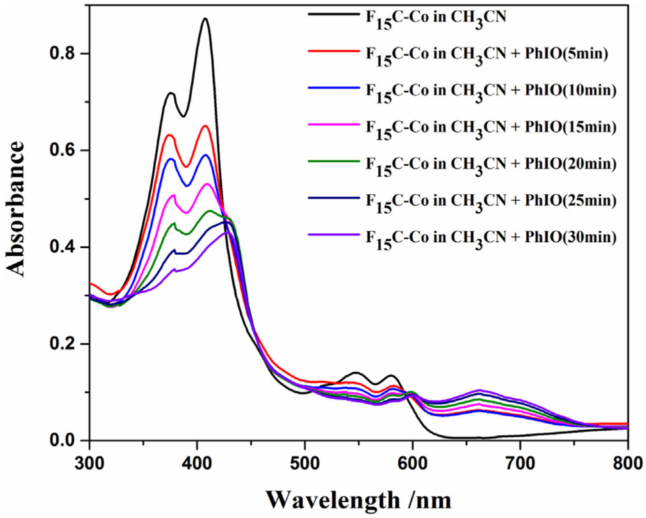

Fig. 7. UV–vis spectral change upon addition of PhIO (8.5 equiv) to a solution of **F_{15}C-Co** in CH_3CN at 25 °C.

Please cite this article in press as: L.-T. Huang, et al., J. Mol. Catal. A: Chem. (2016), http://dx.doi.org/10.1016/j.molcata.2016.11.019

Table 3C
Oxidation of styrene catalyzed by **$Co(OAc)_2 \cdot 4H_2O$** using different oxidants in CH_3CN/H_2O (3:1).

Oxidant	Yield (%)^c					BA^e Selectivity (%)
	BA	PA	SO	TON	Total	
none	0	0	0	0	0	
$PhI(OAc)_2$ ^b	3 (2)	5 (3)	3 (4)	11 (9)	11 (9)	27 (22)
TBHP^a	3 (2)	6 (0)	5 (6)	14 (8)	14 (8)	21 (25)
H_2O_2 ^d	1 (0)	0 (0)	0 (0)	1 (0)	1 (0)	100
$KHSO_5$	1 (0)	1 (0)	1 (2)	3 (2)	3 (2)	33 (0)
PhIO	4(2)	0 (0)	0 (1)	4 (3)	4 (3)	100 (67)
m-CPBA	3 (2)	6 (3)	5 (6)	14 (11)	14 (11)	21 (18)

Note: reaction time: 10 h; an Except for 5 h; b using 0.001 mmol catalyst, 0.1 mmol oxidant, 1 mmol styrene (The molar ratio of catalyst/oxidant/styrene was 1/100/1000); c Yields are based on concentration of oxidant; d Yields in parentheses were obtained in agron condition; e Selectivity of BA is the percentage of BA in total products.

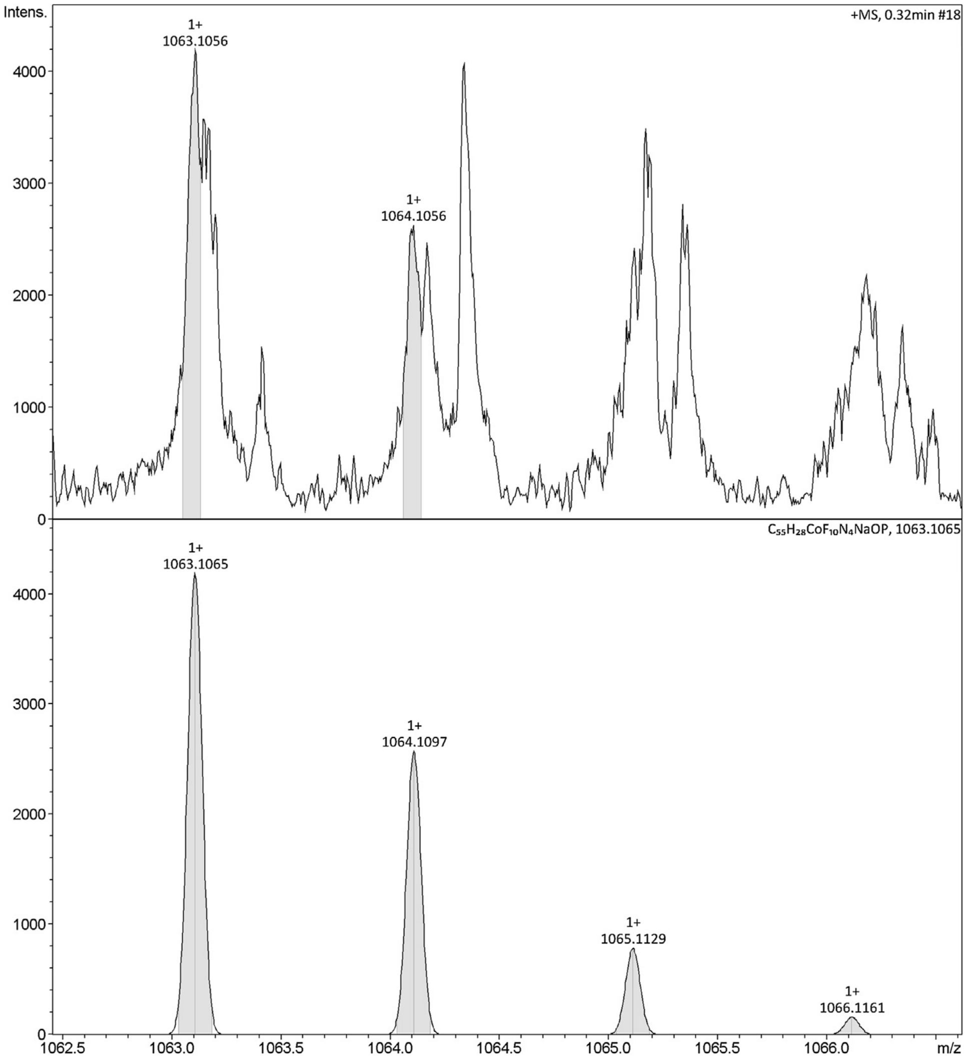

Fig. 5. Situ HR-ESI-MS spectrum of cobalt(III) corrole **F_{10}C-Co** with $KHSO_5$ in CH_3CN.

species with distinct green color change in several minutes and finally were bleached.

The UV–vis spectra of **F_{10}C-Co** upon mixing with styrene in CH_3CN with $KHSO_5$ is demonstrated in Fig. 6. The UV–vis spectras of all four cobalt corroles exhibited similar behaviors in CH_3CN (see Figs. S24–S26 in the Supporting information). The red color changed into green and slight change was observed in both Soret bands and Q bands, but after minutes later both the Soret bands and Q bands of the four cobalt corroles were significantly red-shifted, indicating that existence of an active species expected as the high-valent cobalt corroles. Furthermore, we conducted the situ HR-ESI-MS experiment of styrene oxidation by **F_{10}C-Co** with $KHSO_5$ as oxidant in CH_3CN (Fig. 5). It has been reported that manganese corroles with m-CPBA or PhIO can form the reactive new specie Mn(III)-oxo corrole [2,64,65]. Thus, we presumed that the new species with reactivity is Co(V)-oxo. To further elucidate the state of the new species, we conducted EPR spectroscopy experiment. However, X-band CW EPR Spectroscopy of **F_{10}C-Co** in CH_3CN solution with $KHSO_5$ (103 K) exhibited an electron resonance spectra signal at g = 2.0135 which similar to value reported in the literature of Co(IV) corrole [66] (see Fig. S45 in the Supporting information), which suggested the formation of Co(IV)-oxo. In the absence of

Please cite this article in press as: L.-T. Huang, et al., J. Mol. Catal. A: Chem. (2016), http://dx.doi.org/10.1016/j.molcata.2016.11.019

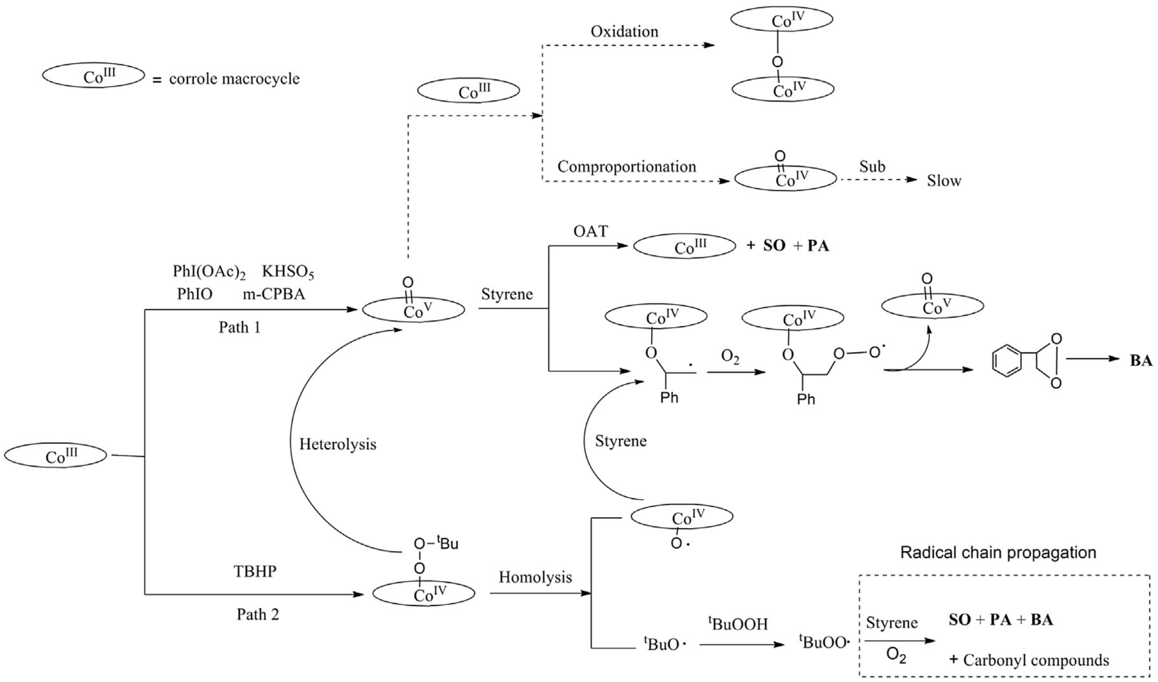

Scheme 3. Plausible mechanism for catalytic oxidation of styrene by cobalt (III) corroles.

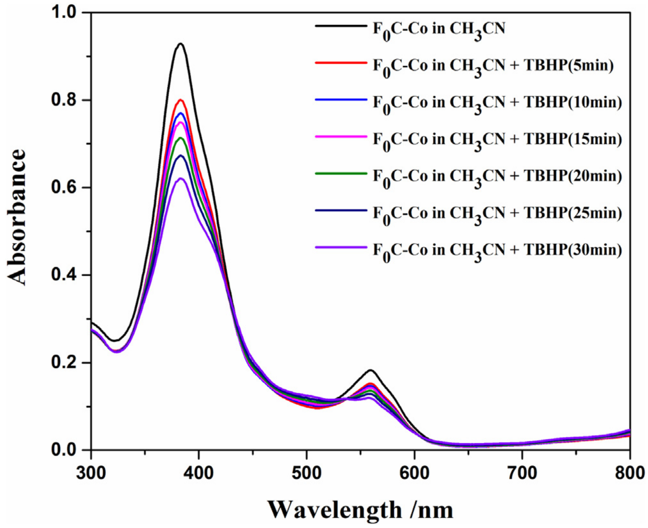

Fig. 8. UV–vis spectral change upon addition of TBHP (8.5 equiv) to a solution of F$_0$**C-Co** in CH$_3$CN at 25 °C.

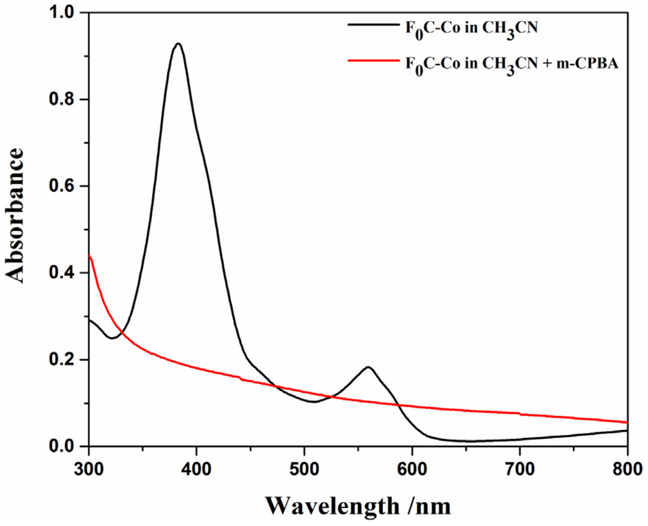

Fig. 9. UV–vis spectral change upon addition of m-CPBA (8.5 equiv) to a solution of F$_0$**C-Co** in CH$_3$CN at 25 °C.

organic substrate, it is possible that the high reactive cobalt(V)-oxo oxidant may react with unreacted cobalt(III) precursor to produce the stable μ-oxo dimer. Other possibility is that cobalt(V)-oxo may react with unreacted cobalt(III) precursor in comproportionation reaction to produce Co(IV)-oxo, which has also been reported in the corrole-iron(V)–oxo species [67,68]. According to the data depicted in Tables 3A and 3B, higher yield which is based on oxidant of benzaldehyde was obtained in the presence of oxygen than in argon atmosphere (see yields in parentheses) when using PhI(OAc)$_2$, KHSO$_5$, PhIO as oxidants, which implies that the formation of benzaldehyde may be attributed to the free radical mechanism with the participation of oxygen catalytic reactions [4,5]. The plausible mechanism is suggested using PhI(OAc)$_2$, KHSO$_5$, PhIO, m-CPBA as oxidant was depicted (Scheme 3. Path 1).

As shown in Figs. 7 and S27–S29 in the Supporting information, when oxidant PhIO was added to cobalt corrole/CH$_3$CN system, all the four cobalt corroles exhibited some similar phenomena as using KHSO$_5$.

Interestingly, when oxidant TBHP was added to a solution CH$_3$CN of cobalt corroles, we could observe slight loss of absorbance in Soret band and Q band for F$_0$**C-Co** (Fig. 8) and other three cobalt corroles (see Figs. S30–S32 in the Supporting information). From the data reflected in Table 3A, we can see that higher total yield which is based on oxidant was obtained in the reaction system cobalt corrole/TBHP/CH$_3$CN in 5 h. Hence, four cobalt complexes exhibited higher catalytic activity when using TBHP as oxidant. When this reaction was carried out in agron, formation of main product benaldehyde was significantly decreased (Table 3A, yields in parentheses). A free-radical reaction that is progagated by the involvement of oxygen led to formation of benzaldehyde, which has been reported previously [4,5]. Thus, plausible mechanism is shown (Scheme 3 Path 2).

Please cite this article in press as: L.-T. Huang, et al., J. Mol. Catal. A: Chem. (2016), http://dx.doi.org/10.1016/j.molcata.2016.11.019

In case of cobalt corrole/m-CPBA/CH_3CN system, as showed in Figs. 9 and S33–S35 in the Supporting information, loss of intensity of the absorption peaks could be observed, which clearly showed that four cobalt (III) corroles were completely bleached upon excess addition of m-CPBA to the solution. The intermediate could not be traced in cobalt corrole/m-CPBA/CH_3CN system. Thus, by combing the data in Table 3B and Fig. 8, we made a conclusion that the stability of four cobalt corroles was poor when m-CPBA was added to the solution, which may account for the fact that m-CPBA inhibited the activity of cobalt corroles. And this was consistent with the result that total yield which is based on oxidant was much lower when using m-CPBA as oxidant reflected in Table 3B.

Combined with the catalytic data shown in Table 3A, the total yield which is based on oxidant was so low that among which benzaldehyde was the major product and no phenylacetaldehyde and styrene epoxide were found in cobalt corroles/H_2O_2/CH_3CN system. It is probably that cobalt corroles hardly work in H_2O_2/CH_3CN system, which means that cobalt corroles cannot effectively catalyze styrene oxidation in this case. Hence, UV–vis spectra of the four catalysts in absence of organic substrate with several equilvalents amount of H_2O_2 added was not carried out.

4. Conclusion

In conclusion, we have prepared a series of cobalt corroles with different electronic structure. They were characterized by UV–vis, NMR, X-ray Photoelectron Spectroscopy and cyclic voltammetry. The catalytic oxidation of styrene by using these cobalt corroles were also carried out. This work revealed that cobalt corroles were potential catalysts for the oxidation of alkene. The solvents, oxidants and electronic structure of cobalt corroles have significant effect on the catalytic oxidation reaction. In CH_3CN solvent, benzaldehyde was found to be the main product when using $PhI(OAc)_2$, TBHP, $KHSO_5$ and PhIO as oxygen source. While styrene epoxide was the major product when using *m*-CPBA oxidant at the conditions. Based on the observations, the catalytic pathway is also discussed. Further investigation on the active intermediate of catalytic oxidation of alkene by cobalt corroles is going on in our laboratory.

Acknowledgement

The financial support from the National Natural Science Foundation of China (21371059, 21671068) is gratefully acknowledged.

Appendix A. Supplementary data

Supplementary data associated with this article can be found, in the online version, at http://dx.doi.org/10.1016/j.molcata.2016.11.019.

References

[1] Z. Gross, H.B. Gray, Adv. Synth. Catal. 346 (2004) 165–170.
[2] Z. Gross, G. Golubkov, L. Simkhovich, Angew. Chem. Int. Ed. 39 (2000) 4045–4047.
[3] H.Y. Liu, H. Zhou, L.Y. Liu, X. Ying, H.F. Jiang, C.K. Chang, Chem. Lett. 36 (2007) 274–275.
[4] Q. Wang, Y. Zhang, L. Yu, H. Yang, M.H. Mahmood, H.Y. Liu, J. Porphyr. Phthalocya. 18 (2014) 316–325.
[5] S.H. Peng, M.H. Mahmood, H.B. Zou, S.B. Yang, H.Y. Liu, J. Mol. Catal. A: Chem. 395 (2014) 180–185.
[6] Z. Gross, N. Galili, L. Simkhovich, I. Saltsman, M. Botoshansky, D. Bläser, R. Boese, I. Goldberg, Org. Lett. 1 (1999) 599–602.
[7] A.N. Biswas, A. Pariyar, S. Bose, P. Das, P. Bandyopadhyay, Catal. Commun. 11 (2010) 1008–1011.
[8] A. Pariyar, S. Bose, A.N. Biswas, P. Das, P. Bandyopadhyay, Catal. Commun. 32 (2013) 23–27.
[9] A.N. Biswas, P. Das, A. Agarwala, D. Bandyopadhyay, P. Bandyopadhyay, J. Mol. Catal. A: Chem. 326 (2010) 94–98.
[10] A. Schechter, M. Stanevsky, A. Mahammed, Z. Gross, Inorg. Chem. 51 (2012) 22–24.
[11] J. Tang, Z. Ou, L. Ye, M. Yuan, Y. Fang, Z. Xue, K.M. Kadish, J. Porphyr. Phthalocya. 18 (2014) 891–898.
[12] K.M. Kadish, L. Frémond, F. Burdet, J.-M. Barbe, C.P. Gros, R. Guilard, J. Inorg. Biochem. 100 (2006) 858–868.
[13] K.M. Kadish, L. Frémond, Z. Ou, J. Shao, C. Shi, F.C. Anson, F. Burdet, C.P. Gros, J.M. Barbe, R. Guilard, J. Am. Chem. Soc. 127 (2005) 5625–5631.
[14] Z. Ou, A. Lü, D. Meng, S. Huang, Y. Fang, G. Lu, K.M. Kadish, Inorg. Chem. 51 (2012) 8890–8896.
[15] B. Li, Z. Ou, D. Meng, J. Tang, Y. Fang, R. Liu, K.M. Kadish, J. Inorg. Biochem. 136 (2014) 130–139.
[16] Z. Wang, H. Lei, R. Cao, M. Zhang, Electrochim. Acta 171 (2015) 81–88.
[17] P. Chattopadhyay, T. Matsuo, T. Tsuji, J. Ohbayashi, T. Hayashi, Organometallics 30 (2011) 1869–1873.
[18] D.K. Dogutan, R. McGuire Jr., D.G. Nocera, J. Am. Chem. Soc. 133 (2011) 9178–9180.
[19] M.Z. Ertem, C.J. Cramer, Dalton Trans. 41 (2012) 12213–12219.
[20] H. Lei, A. Han, F. Li, M. Zhang, Y. Han, P. Du, W. Lai, R. Cao, Phys. Chem. Chem. Phys. 16 (2014) 1883–1893.
[21] B. Mondal, K. Sengupta, A. Rana, A. Mahammed, M. Botoshansky, S.G. Dey, Z. Gross, A. Dey, Inorg. Chem. 52 (2013) 3381–3387.
[22] L.L. Zhou, L.Z. Fu, L.Z. Tang, Y.X. Zhang, S.Z. Zhan, Int. J. Hydrogen Energy 40 (2015) 5099–5105.
[23] L.Z. Fu, L.L. Zhou, L.Z. Tang, Y.X. Zhang, S.Z. Zhan, J. Power Sources 280 (2015) 453–458.
[24] A. Mahammed, B. Mondal, A. Rana, A. Dey, Z. Gross, Chem. Commun. 50 (2014) 2725–2727.
[25] H. Lei, A. Han, F. Li, M. Zhang, Y. Han, P. Du, W. Lai, R. Cao, Phys. Chem. Chem. Phys. 16 (2014) 1883–1893.
[26] J. Grodkowski, P. Neta, E. Fujita, A. Mahammed, L. Simkhovich, Z. Gross, J. Phys. Chem. A 106 (2002) 4772–4778.
[27] K. Peuntinger, T. Lazarides, D. Dafnomili, G. Charalambidis, G. Landrou, A. Kahnt, R.P. Sabatini, D.W. McCamant, D.T. Gryko, A.G. Coutsolelos, J. Phys. Chem. C 117 (2013) 1647–1655.
[28] J.M. Barbe, G. Canard, S. Brandès, R. Guilard, Chem. Eur. J. 13 (2007) 2118–2129.
[29] L. Tortora, G. Pomarico, S. Nardis, E. Martinelli, A. Catini, A. D'Amico, C. Di Natale, R. Paolesse, Sens. Actuators, B 187 (2013) 72–77.
[30] J.M. Barbe, G. Canard, S. Brandès, F. Jérôme, G. Dubois, R. Guilard, Dalton Trans. (2004) 1208–1214.
[31] M.Y. Lee, Y. Chen, X.P. Zhang, Organometallics 22 (2003) 4905–4909.
[32] J. Haber, M. Kłosowski, J. Połtowicz, J. Mol. Catal. A: Chem. 201 (2003) 167–178.
[33] Y. i. Matsushita, T. Matsui, K. Sugamoto, Chem. Lett. (1992) 1381–1384.
[34] J.Y. Liu, X.F. Li, Y.Z. Li, W.B. Chang, A.J. Huang, J. Mol. Catal. A: Chem. 187 (2002) 163–167.
[35] K. E. a. F. M. Lucas HJ, Org. Synth. Wile: N. Y. 3 (1955) pp 483.
[36] D. Nurco, K. Smith, Chem. Commun. (1999) 1307–1308.
[37] D.T. Gryko, B. Koszarna, Org. Biomol. Chem. 1 (2003) 350–357.
[38] B. Koszarna, D.T. Gryko, J. Org. Chem. 71 (2006) 3707–3717.
[39] L. Simkhovich, N. Galili, I. Saltsman, I. Goldberg, Z. Gross, Inorg. Chem. 39 (2000) 2704–2705.
[40] Z. Lei, X. Han, Y. Hu, R. Wang, Y. Wang, J. Appl. Polym. Sci. 75 (2000) 1068–1074.
[41] W. Zhang, A.U. Shaikh, E.Y. Tsui, T.M. Swager, Chem. Mater. 21 (2009) 3234–3241.
[42] D. Hong, J. Jung, J. Park, Y. Yamada, T. Suenobu, Y.M. Lee, W. Nam, S. Fukuzumi, Energy Environ. Sci. 5 (2012) 7606–7616.
[43] R.D. Feltham, P. Brant, J. Am. Chem. Soc. 104 (1982) 641–645.
[44] T. Ivanova, A. Naumkin, A. Sidorov, I. Eremenko, M. Kiskin, J. Electron. Spectrosc. 156 (2007) 200–203.
[45] S. Huang, Y. Fang, A. Lü, G. Lu, Z. Ou, K.M. Kadish, J. Porphyr. Phthalocya. 16 (2012) 958–967.
[46] E. V. C. K.M. Kadish, G. Royal, in: K.M. Kadish, K.M. Smith, R. Guilard (Eds.), The Porphyr. Handbook. 8 (2000) pp. 1–97.
[47] G. R. K.M. Kadish, E. Van Caemelbecke, E. Gueletti, in: K.M. Kadish, K.M., Smith, R.Guilard (Eds.), Academic Press San Diego. 9 (2000) pp. 1–419.
[48] D. Behar, T. Dhanasekaran, P. Neta, C. Hosten, D. Ejeh, P. Hambright, E. Fujita, J. Phys. Chem. A 102 (1998) 2870–2877.
[49] J.H. Furhop, K.M. Kadish, D.G. Davis, J. Am. Chem. Soc. 95 (1973) 5140–5147.
[50] L. Simkhovich, A. Mahammed, I. Goldberg, Z. Gross, Chem. Eur. J. 7 (2001) 1041–1055.
[51] C. Sun, B. Hu, Z. Liu, Chem. Eng. J 232 (2013) 96–103.
[52] Z. Zhang, L. Ouyang, W. Wu, J. Li, Z. Zhang, H. Jiang, J. Org. Chem. 79 (2014) 10734–10742.
[53] M. Zhao, S. Ou, C.-D. Wu, Acc. Chem. Res. 47 (2014) 1199–1207.
[54] T. Michel, D. Betz, M. Cokoja, V. Sieber, F.E. Kühn, J. Mol. Catal. A: Chem. 340 (2011) 9–14.
[55] R.S. Czernuszewicz, V. Mody, A. Czader, M. Gałeñzowski, D.T. Gryko, J. Am. Chem. Soc. 131 (2009) 14214–14215.
[56] V.V. Mody, M.B. Fitzpatrick, S.S. Zabaneh, R.S. Czernuszewicz, M. Gałęzowski, D.T. Gryko, J. Porphyr. Phthalocya. 13 (2009) 1040–1052.
[57] S. Rayati, P. Jafarzadeh, S. Zakavi, Inorg. Chem. Commun. 29 (2013) 40–44.

[58] H. Yang, H.B. Zou, H.H. Wang, S.B. Yang, H. Zhang, H.Y. Liu, Chinese. J. Inorg. Chem. 5 (2015) 968–974.
[59] J.P. Collman, A.S. Chien, T.A. Eberspacher, J.I. Brauman, J. Am. Chem. Soc. 122 (2000) 11098–11100.
[60] J.H. In, S.E. Park, R. Song, W. Nam, Inorg. Chim. Acta 343 (2003) 373–376.
[61] W. Adam, S. Hajra, M. Herderich, C.R. Saha-Möller, Org. Lett. 2 (2000) 2773–2776.
[62] W. Nam, H.J. Han, S.Y. Oh, Y.J. Lee, M.H. Choi, S.Y. Han, C. Kim, S.K. Woo, W. Shin, J. Am. Chem. Soc. 122 (2000) 8677–8684.
[63] J.P. Collman, L. Zeng, R.A. Decréau, Chem. Commun. (2003) 2974–2975.
[64] S. Bose, A. Pariyar, A.N. Biswas, P. Das, P. Bandyopadhyay, Catal. Commun. 12 (2011) 1193–1197.
[65] H.Y. Liu, F. Yam, Y.T. Xie, X.Y. Li, C.K. Chang, J. Am. Chem. Soc. 131 (2009) 12890–12891.
[66] J. Harmer, S. Van Doorslaer, I. Gromov, M. Bröring, G. Jeschke, A. Schweiger, J. Phys Chem B 106 (2002) 2801–2811.
[67] T.H. Chen, K.W. Kwong, A. Carver, W. Luo, R. Zhang, Appl. Catal. A: Gen. 497 (2015) 121–126.
[68] T.H. Chen, K.W. Kwong, N.F. Lee, D. Ranburger, R. Zhang, Inorg. Chim. Acta 451 (2016) 65–72.

Please cite this article in press as: L.-T. Huang, et al., J. Mol. Catal. A: Chem. (2016), http://dx.doi.org/10.1016/j.molcata.2016.11.019